OXFORD

Cerebral Cortex, 2023, 1–11
https://doi.org/10.1093/cercor/bhad372
Original Article

Distinct pre-COVID brain structural signatures in COVID-19-related post-traumatic stress symptoms and post-traumatic growth

Huan Lan[1,2,†], Xueling Suo[1,2,†], Chao Zuo[1,2], Nanfang Pan[1,2], Xun Zhang[1,2], Graham J. Kemp[3], Qiyong Gong[1,4], Song Wang[1,2,*]

[1]Department of Radiology and Huaxi MR Research Center (HMRRC), Functional and Molecular Imaging Key Laboratory of Sichuan Province, West China Hospital, Sichuan University, Chengdu 610041, China,
[2]Research Unit of Psychoradiology, Chinese Academy of Medical Sciences, Chengdu 610041, China,
[3]Liverpool Magnetic Resonance Imaging Centre (LiMRIC) and Institute of Life Course and Medical Sciences, University of Liverpool, Liverpool L69 3BX, United Kingdom,
[4]Department of Radiology, West China Xiamen Hospital of Sichuan University, Xiamen 361000, China

*Corresponding author: Department of Radiology and Huaxi MR Research Center (HMRRC), West China Hospital, Sichuan University, No. 37 Guo Xue Lane, Chengdu 610041, China. Email: wangs_psych@163.com

†Huan Lan and Xueling Suo contributed equally to this work.

Post-traumatic stress symptoms and post-traumatic growth are common co-occurring psychological responses following exposure to traumatic events (such as COVID-19 pandemic), their mutual relationship remains unclear. To explore this relationship, structural magnetic resonance imaging data were acquired from 115 general college students before the COVID-19 pandemic, and follow-up post-traumatic stress symptoms and post-traumatic growth measurements were collected during the pandemic. Voxel-based morphometry was conducted and individual structural covariance networks based on gray matter volume were further analyzed using graph theory and partial least squares correlation. Behavioral correlation found no significant relationship between post-traumatic stress symptoms and post-traumatic growth. Voxel-based morphometry analyses showed that post-traumatic stress symptoms were positively correlated with gray matter volume in medial prefrontal cortex/dorsal anterior cingulate cortex, and post-traumatic growth was negatively correlated with gray matter volume in left dorsolateral prefrontal cortex. Structural covariance network analyses found that post-traumatic stress symptoms were negatively correlated with the local efficiency and clustering coefficient of the network. Moreover, partial least squares correlation showed that post-traumatic stress symptoms were correlated with pronounced nodal properties patterns in default mode, sensory and motor regions, and a marginal correlation of post-traumatic growth with a nodal property pattern in emotion regulation-related regions. This study advances our understanding of the neurobiological substrates of post-traumatic stress symptoms and post-traumatic growth, and suggests that they may have different neuroanatomical features.

Key words: COVID-19; post-traumatic stress symptoms; post-traumatic growth; structural covariance network; psychoradiology.

Introduction

The COVID-19 pandemic has been a serious global health emergency with a profound impact on public mental health (Pfefferbaum and North 2020). It can be considered a traumatic "event" that implies a threat of death or severe injury and evokes many psychological reactions, such as anxiety, fear, and depression (Shanahan et al. 2022; Liu et al. 2023). As a common and negative psychological reaction following the pandemic (Vindegaard and Benros 2020), post-traumatic stress symptoms/disorder (PTSS/PTSD) is characterized by intrusions, avoidance, hyperarousal, and emotional numbing (Pitman et al. 2012). There is increasing evidence of PTSS/PTSD not only in those facing higher levels of exposure to the disease, such as survivors of COVID-19 or healthcare workers (Carmassi et al. 2020; Tu et al. 2021), but also in the general population (Rossi et al. 2020; Wang et al. 2020a), which has important implications for public mental health (Brooks et al. 2020). Nevertheless, similar to many other traumatic events, the COVID-19 pandemic can also result in positive psychological response such as post-traumatic growth (PTG) (Mo et al. 2021; Wang et al. 2023), which refers to the experience of positive psychological change resulting from the struggle with challenging life crises or stressful events (Tedeschi and Calhoun 2004).

Because PTSS and PTG often coexist in individuals experiencing trauma (Dekel et al. 2012; Wu et al. 2016; Pietrzak et al. 2021), studies have attempted to elucidate the relationship between them. These have yielded inconsistent results: some studies report a positive correlation (Solomon and Dekel 2007; Jin et al. 2014; Groarke et al. 2017; Logue et al. 2018), some a negative correlation (Wu et al. 2016), and others find no correlation (Cordova et al. 2001; Shand et al. 2015; Wei et al. 2017b); there is some evidence for an inverted "U" association, indicating the presence of a moderate level of PTSS, corresponding to the highest level of PTG (Shakespeare-Finch and Lurie-Beck 2014; Tsai et al. 2015). These mixed results could be caused by factors such as diverse sample characteristics, heterogeneity with regard to trauma type and severity, and different measurements and study methods (Shakespeare-Finch and Lurie-Beck 2014; Shand et al. 2015; Marziliano et al. 2020). A more general factor is the limited reproducibility of current psychological science (Nosek et al. 2022) and in particular the proneness of behavioral self-reported tests to methodological bias (Podsakoff et al. 2003). Potential clarity

Received: August 8, 2023. **Revised:** September 12, 2023. **Accepted:** September 13, 2023

may result from neuroscience approaches, in which brain data are used to explore the underlying neurobiological substrates of individual differences in human cognitions, affects, and behaviors (Foulkes and Blakemore 2018; Genon et al. 2022; Lin et al. 2023).

Previous structural neuroimaging studies have provided some insights into the neural basis of PTSD/PTSS, not only involving changes in discrete brain regions [e.g. gray matter (GM) changes in prefrontal cortex (PFC) and limbic regions (Bromis et al. 2018; Li et al. 2022b)], but increasingly characterized by altered networks of brain structures (Harnett et al. 2022). Prefrontal-limbic structural alterations are predictive for differences and severity of PTSS among different populations (Carrion et al. 2010; Balters et al. 2021). Besides, individuals with reduced structural covariance network (SCN) intensity of ventral visual flow over time generally had higher PTSD symptom severity (Harnett et al. 2022). Conversely, the neuroanatomy of PTG is less well studied. As we know, only one study analyzed its link to brain structure, finding that in individuals who experienced the East Japan Great Earthquake, PTG levels were positively associated with increased GM volume (GMV) in the right dorsolateral prefrontal cortex (DLPFC) compared with measurements made 3 months pre-earthquake (Nakagawa et al. 2016). A functional neural network study revealed a positive association of PTG with the brain activation in central executive network (Fujisawa et al. 2015). Despite extensive investigations toward underlying brain mechanisms of post-traumatic related issues, the neurobiological correlates of PTSS and PTG during the pandemic are poorly understood. Regarding individual variations in post-traumatic impacts among general public during the pandemic (Schou et al. 2021), probing corresponding brain markers could help identify those vulnerable individuals and develop targeting preventive measures.

As a promising research direction, structural MRI (sMRI) can be used not only to evaluate GMV at the voxel level, but also SCN formed according to morphological associations, enabling the analysis of the relationship between the brain and behavior at the individual level (Cai et al. 2023; Lai et al. 2023). There are evidences that diversity in structural covariance patterns between individuals is responsible for cognitive, affective, and behavioral differences (Khundrakpam et al. 2017; Lu et al. 2023). Thus, combining the methods of GMV and SCN based on sMRI to identify local and structural network signatures associated with PTSS/PTG will help us comprehensively understand their neuroanatomical basis and the nature of individual differences in post-traumatic psychological responses related to the pandemic.

To this end, we first conducted behavioral correlation analyses to investigate the relation between PTSS and PTG during the COVID-19 pandemic. Then, whole-brain correlation analyses based on voxel-based morphometry (VBM) approach (Ashburner and Friston 2000) were conducted to determine the brain regions whose GMV associated with PTSS and PTG, respectively. Furthermore, for each participant, a whole-brain SCN approach was applied to quantitatively assess structural covariance between each pair of brain areas. Each individual GM covariance network was characterized using graph theoretical method, and common graph metrics were examined. Finally, partial correlation and partial least squares correlation (PLSC) were conducted to identify the patterns of GM covariance network related to PTSS/PTG. Because no study has yet examined the neural link between PTSS and PTG, our conjunction analyses were exploratory.

Methods and materials

Participants

A total of 151 general individuals with no history of neuropsychiatric disease were recruited from a larger project aimed at exploring the neuropsychology of personality and mental health (Lai et al. 2022; Pan et al. 2022; Suo et al. 2022). These participants had completed pre-pandemic brain scanning from October 2019 to January 2020 (T1, before China declared a state of emergency and a nationwide lockdown). All participants were re-contacted for the second stage of post-traumatic behavioral evaluations during the first outbreak and peak period from February to April 2020 (T2, the worst period of the pandemic in China), and 127 participants replied and finished the examinations. Of those, 12 participants were excluded for failing to pass the fake items that are either obvious or ridiculous. For estimation of sample size, since a minimum of 84 participants are required to identify medium-sized effects for performing correlation analyses ($r = 0.3$, $\alpha = 0.05$, $1\text{-}\beta = 0.80$) according to standard power analysis (Faul et al. 2007; Suo et al. 2022), our main purpose was to recruit ~100 participants. Finally, 115 participants (49 males, 66 females, mean age = 22.37, standard deviation, SD = 2.07) were included in the subsequent data analyses. COVID-19 Polymerase Chain Reaction testing showed that no participants were positive at T2 stage. Notably, several other analyses on these participants have been performed (e.g. analyses on functional connectome (Pan et al. 2022; Suo et al. 2022), with the results reported in the cited papers. The local research ethics committee of West China Hospital of Sichuan University approved the research protocol and we obtained written informed consent from each participant at each stage in line with the Declaration of Helsinki.

Behavioral measures

Impact of event scale-revised

To evaluate individuals' levels of PTSS we used the impact of event scale-revised (IES-R), a widely used instrument for assessing subjective distress caused by traumatic events (Creamer et al. 2003). The IES-R contains 22 items and 3 subscales (8 items for intrusions, 8 for avoidance, and 6 for hyperarousal). Each participant was asked to confirm a specific stressful life event (in this case the COVID-19 pandemic) and indicate how much distress or bother they felt for each of difficulty listed. Items are scored on a 5-point Likert scale ranging from 1 ("not at all") to 5 ("extremely"), with a higher score representing more severe PTSS. The Chinese version of IES-R has been well-validated and widely used for investigating pandemic-specific PTSS (Peng et al. 2020; Wang et al. 2020a). In the present sample, Cronbach's α for IES-R was 0.89, indicating satisfactory internal reliability.

Post-traumatic growth inventory

To measure individual differences in PTG, we adopted the Chinese version of PTGI (Ho et al. 2004), which was originally developed by Tedeschi and Calhoun (Tedeschi and Calhoun 1996). The PTGI is a multidimensional measure with 21 items in 5 areas, including new possibilities (5 items), relating to others (7 items), personal strength (4 items), spiritual change (2 items), and appreciation of life (3 items), and uses a 6-point Likert scale with response format ranging from 1 to 6. The entire score of all items represents the PTGI score, a higher score indicating a higher level of PTG. The Chinese version of PTGI exhibits good reliability and validity for assessing PTG related to COVID-19 (Yan et al. 2021; Li et al. 2022a).

The Cronbach's α for PTGI was 0.97 in the present sample, suggesting excellent internal reliability.

MRI data acquisition and preprocessing

Data acquisition

The sMRI data were acquired using a 3.0 T Siemens-Trio Erlangen scanner with a 12-channel head coil. High-resolution T1-weighted anatomical images were acquired on a rapid gradient-echo planar imaging sequence. The parameters are as follows: slice 176, voxel size $1 \times 1 \times 1$ mm^3, matrix size 256×256, slice thickness 1 mm, flip angle 9°, repetition time 1900 ms, inversion time 900 ms, and echo time 2.26 ms.

Data preprocessing

We employed an improved and standardized VBM approach to assess regional GMV (Ashburner and Friston 2000), a well-validated generic parameter for describing GM morphology that has been greatly used to investigate the neurobiological bases of human cognitions, affects, personalities, and behaviors (Kanai and Rees 2011; Pan et al. 2021). We preprocessed the images using the automated Computational Anatomy Toolbox (CAT12, http://dbm.neuro.uni-jena.de/cat12/) on statistical parameter mapping (SPM12) in MATLAB (r2013b). Specifically, in SPM12, the images were first reoriented to the anterior commissure for better registration, and then were segmented into GM, white matter, cerebrospinal fluid probability plot and background using ICBM tissue probability atlases. Morphological and anatomical registration, normalization and modulation analysis were then performed by Diffeomorphic Anatomical Registration Through Exponentiated Lie algebra (DARTEL) (Ashburner 2007). Gray matter images were aligned and resampled to $1.5 \times 1.5 \times 1.5$ mm^3 and normalized to Montreal Neurological Institute (MNI152) space. The segmented GM was modulated using the local transformation inverse Jacobian matrix to preserve the volume measurement. Finally, the modulated GMV images were smoothed using a full-width at half-maximum Gaussian kernel of 8 mm.

Network construction and analysis

We identified the 90 regions of interest segmented by whole brain GM as nodes via Automated Anatomical Labeling (AAL) atlas (Tzourio-Mazoyer et al. 2002), and interregional connections as edges via Kullback–Leibler divergence-based similarity (KLS) method (Wang et al. 2016). Briefly, we extracted the GMV values of all voxels in each ROI for each participant and applied kernel density estimation to evaluate their probability density function to calculate the probability distribution function (PDF). Then, Kullback–Leibler divergence was calculated among all ROI pairs in the PDFs, and KLS values were calculated across all probable brain region pairs, which range from 0 to 1, with 1 representing two equal distributions. Finally, we obtained 90×90 morphological connection matrix based on KLS for each participant. To assure that morphological networks have equal number of edges, we applied a broad range of sparsity (S) thresholds ($0.05 \leq S \leq 0.28$ with steps of 0.01) to each matrix (Zhang et al. 2011).

We used GRETNA software to perform graph theoretical analyses of GM networks (Wang et al. 2015). We estimated commonly used graph metrics including global (global efficiency, characteristic path length and normalized characteristic path length, small worldness, local efficiency, clustering coefficient, and normalized clustering coefficient) and regional (nodal local efficiency, nodal clustering coefficient, and nodal betweenness centrality) properties of these constructed networks. Area under the curve for each network measurement was calculated across S thresholds to offer a summary measure (Zhang et al. 2011).

Statistical analyses

Behavioral analyses

Using the IBM SPSS Statistics 22.0, descriptive statistics and bivariate correlation coefficients were calculated for study measures, and independent samples *t*-tests were performed to test the sex differences.

GMV-behavior correlation analyses

Whole-brain voxel-wise correlation analyses were conducted to detect brain areas in which GMV was associated with PTSS and PTG. The IES-R or PTGI scores were considered the variable of interest and age, sex and total intracranial volume (TIV) were controlling variables. In addition, to investigate sex differences in the association between PTSS/PTG and GMV, we conducted a condition-by-covariate interaction analysis (Yamasue et al. 2008; Wang et al. 2018; Pan et al. 2023) with sex as a condition, PTSS/PTG score as a covariate of interest, age and TIV as covariates of no interest. An absolute threshold masking of 0.2 was applied to remove the edge effect around gray and white matter boundaries. The Gaussian random field approach was used to determine the regions of significance (Worsley et al. 1992), taking a threshold of $P < 0.001$ at the voxel level and $P < 0.05$ at the cluster level, which is a reliable correction method for VBM data (Qiu et al. 2018; Wang et al. 2020b).

Network-based statistical analyses

The relationships between global metrics and PTSS/PTG were analyzed using partial correlations, with age, sex, and TIV as covariates. Bonferroni correction for multiple comparisons was performed to maintain a significant level of $P < 0.05$. The relationships between the pattern of nodal metrics and PTSS/PTG were analyzed using a multivariate statistical method named PLSC, which has been widely used and successfully validated in previous studies and its advantageous features have also been reported elsewhere (Jessen et al. 2019; Lai et al. 2022). We used a PLS toolbox in MATLAB r2013b for PLSC. This approach aims to identify latent variables that describe patterns of brain measures that maximally covary with behavioral or task characteristics (Krishnan et al. 2011). Concretely, we first regressed out the influence of confounding factors (sex, age, and TIV) on each node attributes and PTSS/PTG. The residuals obtained were then used for PLSC, mainly including three steps suggested by Krishnan et al. (Krishnan et al. 2011). First, the singular value decomposition (SVD) was used to divide the interindividual correlation matrix (X^TY) between nodal properties (X: 114×90) and PTSS/PTG (Y: 114×1) into three matrices, i.e. U [the left singular vector (90×1) implying the weight of each node on the latent variable of nodal metrics], V [the right singular vector (1×1) for calculating the latent variable of PTSS/PTG; here equal to 1], and $\mathbf{\Sigma}$ [the singular value vector (1×1) implying the largest covariance between the two potential variables]; hence, each participant will be given a latent variable scores ($X \times U$) describing the nodal metrics pattern that is maximally correlated with PTSS/PTG, with higher scores indicating stronger performance for this PTSS/PTG related nodal pattern. Second, permutation tests were applied to detect whether the latent variable of node is applicable to other populations or statistically significant. SVDs were re-executed on a permutation sample, where the matrix X was casually reordered

Table 1. Descriptive statistics and bivariate correlations of study variables.

Variables	Mean ± SD	Range	1	2	3	4	5
Sex[a]	-	-	-				
Age (y)	22.37 ± 2.07	19–27	−0.10	-			
TIV (ml)	1478 ± 123	1251–1778	−0.67*	0.05	-		
PTSS	28.89 ± 7.27	22–60	0.11	−0.02	−0.10	-	
PTG	62.83 ± 23.19	21–121	0.01	−0.20*	−0.06	0.10	-

Abbreviations: y, years; SD, standard deviation; PTSS, post-traumatic stress symptoms; PTG, post-traumatic growth; TIV, total intracranial volume. $*P < 0.05$.
[a]Male, 0; Female, 1.

5,000 times, while the matrix Y was unchanged to acquire a random distribution of singular values (Σ); the latent variables determined in prior step were deemed statistically significant if the practical singular value is greater than at least 95% of the singular value in random distribution. Third, in assessing which nodes contribute robustly to the node's latent variable, we re-ran SVDs on a bootstrap sample, where a random weight distribution for each node was generated by the data in matrices X and Y being resampled and replaced 5,000 times, from which we estimated standard error of each weight. When the actual normalized weight of a node (that is, actual weight divided by its standard error; comparable with a Z score) is >2, it can be considered that the node weight has a robust contribution to the latent variable (Krishnan et al. 2011), indicating that it plays a key role in the PTSS/PTG related pattern of the corresponding node attributes.

Results

Behavioral characteristics of PTSS and PTG during the pandemic

Table 1 shows the descriptive statistics and bivariate correlations of the study variables. The mean score (SD) for IES-R scale was 28.89 (7.27), and the mean score for PTGI was 62.83 (23.19). The levels of PTSS/PTG in the present study are comparable with those from previous studies in Chinese populations related to COVID-19 [e.g. PTSS: 14.32 (10.48)-32.98 (11.69) (Peng et al. 2020; Wang et al. 2020a; Ke et al. 2022); PTG: 59.77 (22.29)-70.53 (17.26) (Cui et al. 2021; Li et al. 2022a)]. There were no sex differences in PTSS ($t[113] = 1.20$, $P = 0.232$) or PTG ($t[113] = 0.05$, $P = 0.962$). Participants' age was negatively correlated with PTG ($r = -0.20$, $P = 0.029$), but not with PTSS ($r = -0.02$, $P = 0.821$). TIV was not correlated with PTG ($r = -0.06$, $P = 0.504$) or PTSS ($r = -0.10$, $P = 0.283$). Importantly, we observed no significant association between PTSS and PTG ($r = 0.10$, $P = 0.292$), or after adjusting for sex, age, and TIV ($r = 0.10$, $P = 0.311$).

GMV related to PTSS/PTG during the pandemic

In whole-brain correlation analysis, after controlling for sex, age, and TIV, PTSS was positively associated with GMV in the left medial prefrontal cortex extending to dorsal anterior cingulate cortex (MPFC/dACC; Table 2 and Fig. 1); PTG was negatively associated with GMV in the left DLPFC [from middle frontal gyrus (MFG) extending to superior frontal gyrus; Table 2 and Fig. 1]. To check their specificity, including PTG as an additional controlling variable, PTSS was still associated with GMV in the left MPFC/dACC (Table 2); including PTSS as an additional controlling variable, PTG was still associated with GMV in the left DLPFC (Table 2). In addition, we found no significant regions for the interaction effect of PTSS/PTG by sex via condition-by-covariate interaction analysis.

Patterns of SCNs linked to PTSS/PTG during the pandemic

After adjusting for age, sex, and TIV, partial correlations showed that PTSS was negatively associated with local efficiency ($r = -0.31$, $P = 0.007$, after Bonferroni correction) and clustering coefficient ($r = -0.29$, $P = 0.014$, after Bonferroni correction) of the network (Fig. S1). There were no significant relations between PTSS and global efficiency, characteristic path length, normalized characteristic path length, small-worldness or normalized clustering coefficient after Bonferroni correction (all $|rs| < 0.17$, all $Ps > 0.574$). No significant correlation was found between PTG and global network metrics after Bonferroni correction (all $|rs| < 0.14$, all $Ps > 0.994$).

PLSC showed a significant latent variable that included a nodal local efficiency and nodal clustering coefficient pattern linked to PTSS, respectively. The pattern of nodal local efficiency ($r = 0.63$, $P = 0.012$) and nodal clustering coefficient ($r = 0.67$, $P = 0.012$) positively covaried with PTSS (Fig. 2A and B). In addition, PLSC revealed a potential variable that was marginally significant, consisting of a nodal betweenness centrality pattern that was positively covaried with PTG ($r = 0.65$, $P = 0.063$) (Fig. 2C). The bootstrap approach further denoted that in the nodal local efficiency pattern of PTSS, four nodes had positive contributions, including left inferior parietal lobule (IPL, including supramarginal and angular gyrus), left parahippocampal gyrus, left amygdala, right MFG; four nodes had negative contributions, including left paracentral lobule (PCL), right Heschl gyrus (HES), right inferior occipital gyrus (IOG), left angular gyrus (ANG). In the nodal clustering coefficient pattern of PTSS, two nodes had positive contributions, including left IPL and fusiform gyrus (FG); five nodes had negative contributions, including right inferior frontal gyrus, opercular part (IFGoperc), left rolandic operculum (ROL), right HES, right IOG, left PCL. In addition, in the betweenness centrality pattern of PTG, seven nodes had positive contributions, including right superior frontal gyrus, orbital part (ORBsup), left HES, left median cingulate and paracingulate gyri (MCG), right precentral gyrus (PreCG), right olfactory cortex, right ANG, right insula; two nodes had negative contributions, including left supplementary motor area (SMA) and middle temporal gyrus (MTG). The standardized weights for each node are reported in Table 3.

Discussion

In this prospective study, we collected behavioral data (i.e. PTSS and PTG) during the period of community-level outbreak of a group of college students who had achieved brain MRI scans before the pandemic. We investigated the behavioral relation between PTSS and PTG and found that there was no significant association. Using sMRI, the regional structure and topological characteristics of morphological networks associated with PTSS

Table 2. Brain regions where GMV is significantly related to PTSS and PTG.

Post-traumatic response	Controlling variables	Brain region	No. of voxels	BA	Peak t score	Peak MNI coordinates		
						X	Y	Z
PTSS	Age, sex, and TIV	Left MPFC/dACC	203	BA6/32	3.75	−10	45	18
	Age, sex, TIV, and PTG	Left MPFC/dACC	222	BA6/32	3.76	−11	45	18
PTG	Age, sex, and TIV	Left DLPFC	248	BA8/9	−4.31	−21	23	45
	Age, sex, TIV, and PTSS	Left DLPFC	234	BA8/9	−4.27	−21	23	45

Abbreviations: BA, Brodmann area; dACC, dorsal anterior cingulate cortex; DLPFC, dorsolateral prefrontal cortex; MPFC, medial prefrontal cortex; MNI, Montreal Neurological Institute; PTG, post-traumatic growth; PTSS, post-traumatic stress symptoms; TIV, total intracranial volume.

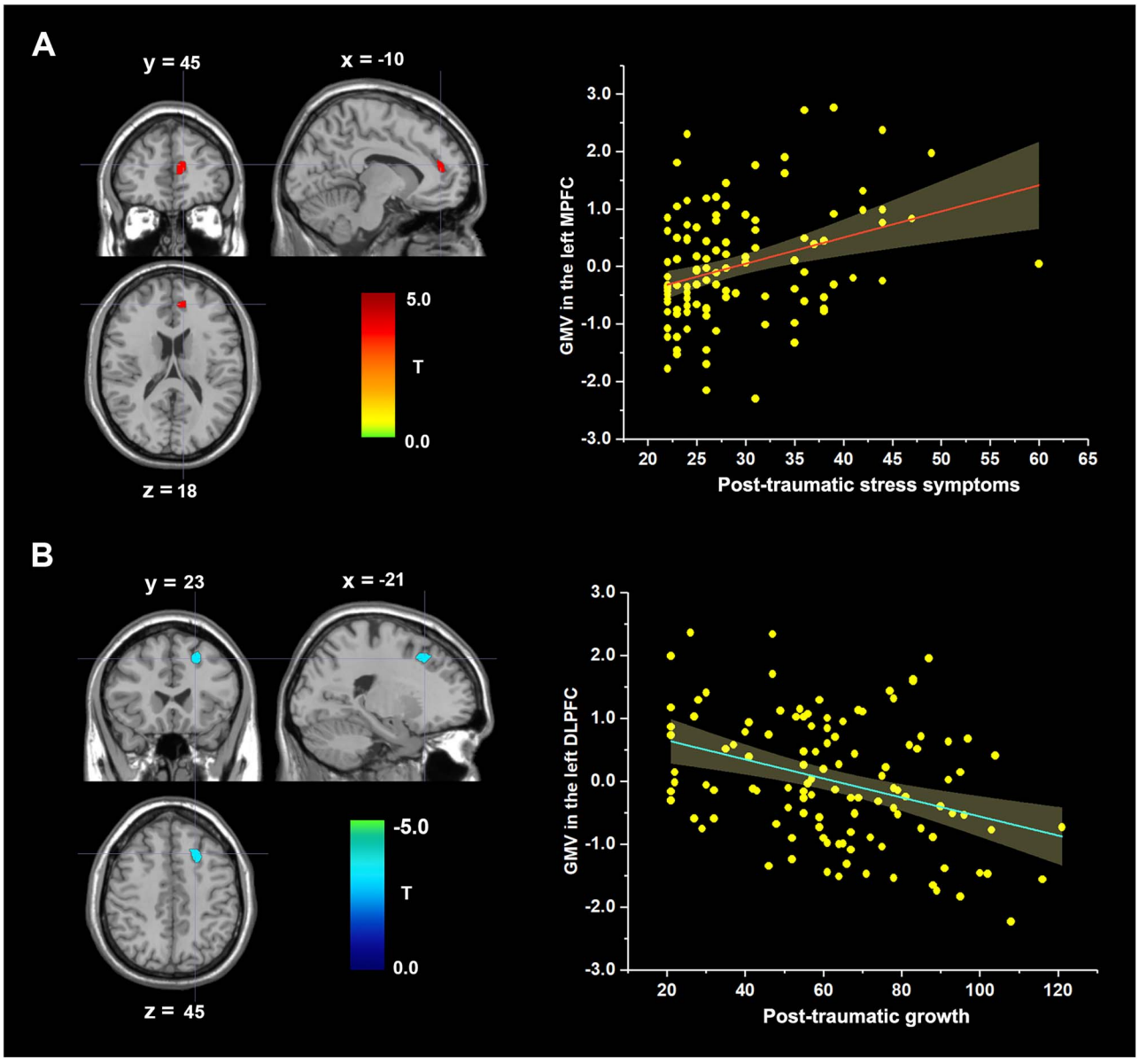

Fig. 1. Regional GMV related to PTSS/PTG. The left side shows brain images, the right side shows scatter plots, and the scores on the y-axis represent the standardized residuals of the GMV values after sex, age, and TIV were regressed out. (A) PTSS is positively linked with GMV in the left MPFC after adjusting for sex, age, and TIV. (B) PTG is negatively linked with GMV in the left DLPFC after adjusting for sex, age, and TIV. Abbreviations: DLPFC, dorsolateral prefrontal cortex; GMV, gray matter volume; MPFC, medial prefrontal cortex.

and PTG were calculated. The current study is the first investigation to incorporate the GMV and SCNs of PTSS and PTG simultaneously in the context of the pandemic, and suggests that PTSS and PTG have different brain-related substrates at the regional level and network level. We now discuss the implications in more detail.

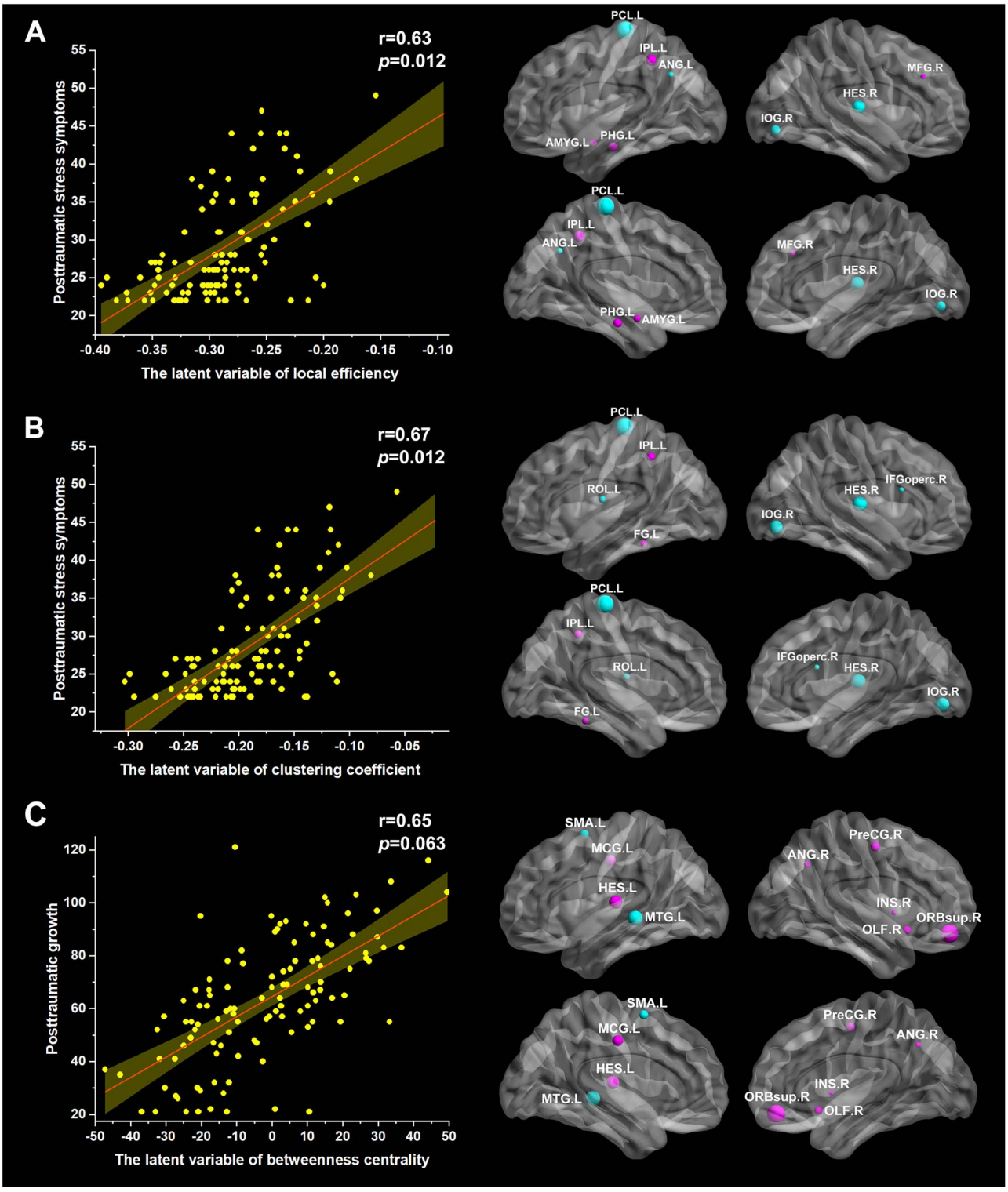

Fig. 2. The relationships between nodal attributes and PTSS/PTG. The results were visualized using BrainNet viewer (http://www.nitrc.org/projects/bnv). Panel (A) shows that PTSS was positively linked to a latent variable that comprised a nodal local efficiency pattern of the network. Panel (B) shows that PTSS was positively linked to a latent variable that comprised a nodal clustering coefficient pattern of the network. Panel (C) shows that PTG was positively linked to a latent variable that comprised a betweenness centrality pattern of the network. The brain images show the bootstrap standardized weight of each region on the identified latent variables, with positive and negative contributions to the patterns. Abbreviations: L, left; R, right; AMYG, amygdala; ANG, angular gyrus; FG, fusiform gyrus; HES, Heschl gyrus; IFGoperc, inferior frontal gyrus, opercular part; INS, insula; IOG, inferior occipital gyrus; IPL, inferior parietal lobule; MCG, median cingulate and paracingulate gyri; MFG, middle frontal gyrus; MTG, middle temporal gyrus; OLF, olfactory cortex; ORBsup, superior frontal gyrus, orbital part; PCL, paracentral lobule; PHG, parahippocampal gyrus; PreCG, precentral gyrus; ROL, rolandic operculum; SMA, supplementary motor area.

Table 3. The bootstrap standardized weight of each node on the latent variables of PTSS and PTG.

L/R	Nodes	Standardized weight
Local efficiency (PTSS)		
L	Inferior parietal, but supramarginal and angular gyri	3.157
L	Parahippocampal gyrus	2.822
L	Amygdala	2.342
R	Middle frontal gyrus	2.022
L	Paracentral lobule	−4.644
R	Heschl gyrus	−3.650
R	Inferior occipital gyrus	−3.023
L	Angular gyrus	−2.179
Clustering coefficient (PTSS)		
L	Inferior parietal, but supramarginal and angular gyri	2.671
L	Fusiform gyrus	2.307
L	Paracentral lobule	−4.642
R	Heschl gyrus	−3.938
R	Inferior occipital gyrus	−3.767
L	Rolandic operculum	−2.374
R	Inferior frontal gyrus, opercular part	−2.006
Betweenness centrality (PTG)		
R	Superior frontal gyrus, orbital part	2.724
L	Heschl gyrus	2.446
L	Median cingulate and paracingulate gyri	2.305
R	Precental gyrus	2.225
R	Olfactory cortex	2.158
R	Angular gyrus	2.209
R	Insula	2.002
L	Middle temporal gyrus	−2.525
L	Supplementary motor area	−2.212

Abbreviations: L, left; R, right; PTG, post-traumatic growth; PTSS, post-traumatic stress symptoms.

The lack of behavioral association between PTSS and PTG fits with previous findings (Cordova et al. 2001; Shand et al. 2015). This relationship is known to be affected by factors such as trauma exposure levels, trauma type, and age (Shakespeare-Finch and Lurie-Beck 2014; Shand et al. 2015; Liu et al. 2017); for example, compared with higher levels of trauma exposure, a lower level may weaken the association of PTSS and PTG (Wei et al. 2017b), which may be why it is stronger in natural disaster survivors or health professionals who assist trauma survivors (Shakespeare-Finch and Lurie-Beck 2014); furthermore, the association of PTSS and PTG is stronger in children than in adults (Shakespeare-Finch and Lurie-Beck 2014). Note that our participants were healthy young adults and their trauma exposure levels were relatively low.

The positive association between PTSS and GMV in left MPFC/dACC is consistent with studies showing increased GMV (Zhang et al. 2018) and cortical thickness (Li et al. 2022b) of the MPFC/dACC in PTSD patients in relative to healthy controls. As a core component of the default-mode network (DMN), MPFC/dACC is related to self-referential processing, inhibition control, and top–down emotion regulation (Patel et al. 2012; Alexandra Kredlow et al. 2022). Neurocircuitry models of PTSD posit that MPFC/dACC fails to inhibit the amygdala, resulting in attentional bias to threats, increased fear responses and deficits in top–down emotion regulation (Elzinga and Bremner 2002; Rauch et al. 2006). Functional neuroimaging studies in PTSS find increased activation in the MPFC/dACC during relevant tasks, suggesting a failing attempt at compensatory suppression of adverse emotional responses (Carrion et al. 2008; Garrett et al. 2012), and our positive correlation between PTSS and left MPFC/dACC GMV may be the structural manifestation of this (Herringa et al. 2013; Jeong et al. 2021).

In addition, at the network level, we found that PTSS was negatively correlated with local efficiency and clustering coefficient in interregional SCNs. Local efficiency and clustering coefficient mainly reflect the network segregation of the human brain (Bullmore and Sporns 2012). Individuals with higher PTSS scores had reduced network segregation in our study, indicating that individuals' GM networks may shift toward to a more random organization. A similar network segregation has been observed in other stress-related conditions, such as trauma-exposed controls, and this randomization process is thought to possibly reflect a compensatory adaptation of brain networks when facing of trauma to cope with the impact of the disease (Xu et al. 2022). Another significant finding of our study is that we observed a nodal local efficiency and nodal clustering coefficient pattern in the GM covariance network associated with PTSS. Among them, brain regions with positive contributions were predominantly located in DMN including left IPL, parahippocampus, FG, and right MFG, which is involving in self-referential processing and episodic memory (Smallwood et al. 2021). Altered DMN connectivity has been widely reported in PTSD, and deficits in DMN are related to PTSD symptoms, such as inability to maintain a stable internal state (e.g. intrusive symptoms), generalization of fear (e.g. avoidance), and altered sense of self-world (e.g. dissociation) (Akiki et al. 2017). The increased node properties of DMN regions found in our study suggest their greater potential in coordinating the large network, which may improve the resistance of network topology to some extent, thereby reducing the damage from COVID-19 stressor in integrating self-referential information. Besides, we found brain regions with negative contributions were mainly located in sensory and motor areas, including left ANG, PCL, rolandic operculum, right IOG, HES, and IFGoperc. Consistent with PTSD functional network studies, alterations in these nodes

are a common aspect of functional network disruption (Bao et al. 2021), which may imply a decrease sensorimotor cortical integration and a reduced role in global network information processing.

For PTG, the GMV of DLPFC associated with it is in line with prior neuroimaging studies (Fujisawa et al. 2015; Wei et al. 2017a). The DLPFC sends afferent projections to subcortical structures such as striatum, hippocampus, and amygdala, and is involved in higher-order cognitive processes such as conscious decision-making, cognitive control, as well as emotional regulation (MacDonald et al. 2000; Krawczyk 2002; Badre and Wagner 2004). This aligns with the neurocircuitry model of PTG, which highlights the role of higher-order cognitive processing in individuals struggling with challenging life circumstances (Tedeschi and Calhoun 2004). Lower PTSD symptom severity and better recovery and resilience have been linked with DLPFC activation and morphology (Lyoo et al. 2011; Aupperle et al. 2012). Repetitive transcranial magnetic stimulation of left DLPFC decreases core PTSD symptoms (avoidance and re-experiencing) and benefits mood (Boggio et al. 2010). If the DLPFC is indeed involved in positive psychological changes in individuals experiencing trauma, the negative association between PTG and left DLPFC GMV may reflect increased myelination and synaptic pruning (Sowell et al. 2001; Paus 2005). This is supported by reports that the volume of left DLPFC is negatively correlated with positive psychological constructs such as "grit" personality (Wang et al. 2018), social well-being (Kong et al. 2015), and elevation tendency (Liu et al. 2018).

Furthermore, our examination of PTG revealed a tendency of positive covariation with a nodal betweenness centrality pattern. That is to say, the more pronounced this centrality pattern is in an individual, the higher the PTG level. This centrality pattern consists of nine regions (i.e. right ORBsup, PreCG, olfactory cortex, ANG, insula, left HES, MCG, SMA, and MTG, seven with positive contributions and two with negative contributions, Table 3). Interestingly, most of these regions are crucial to emotion regulation (Morawetz et al. 2020; Pozzi et al. 2021). Effective emotion regulation has been associated with many positive outcomes, such as an increase in general well-being, better personal and professional relations, and higher levels of mental and physical health (Gross and John 2003). In contrast, deficits in emotion regulation may lead to many psychological problems and psychiatric disorders such as depression and anxiety (Kaiser et al. 2015). Thus, the centrality pattern linked to PTG may reflect the greater potential of these regions to influence emotion regulation-related processing, allowing for more effective coordination and thereby benefitting the development of PTG.

Our research has several limitations. First, our findings presented can be categorized as brain-wide associations (BWAS), and the recent evidence (Marek et al. 2022) suggests that reproducible BWAS require thousands of individuals. In the light of a relatively small single sample of general college students, the current findings need to be interpreted with caution and more works with larger sample sizes are warranted. Also, our results are not necessarily applicable to highly vulnerable groups (e.g. frontline medical workers) and other general public populations (e.g. children and the elderly). Second, we only performed MRI scan and behavioral measures once before and during the pandemic. A longitudinal design with brain and behavioral measurements at multiple time points will be needed to test and extend our results. Third, since graph terminology is originally used to characterize functional network, certain caution is necessary in interpreting this methodology when applying it to the SCN. Besides, there is no widely accepted optimal way to define nodes and edges. We took the AAL template regions as nodes and interregional similarity in the GMV distributions as edges for network construction. We made a conservative choice in methodology as AAL template is used for most work. It will be interesting to study other node definitions or morphological features and techniques (e.g. cortical thickness, functional MRI, diffusion tensor imaging) to explore the biological mechanisms underlying post-traumatic outcomes.

In conclusion, this prospective study demonstrates that there are distinct GM structure and morphological network patterns in PTSS and PTG related to COVID-19. PTSS was correlated with GMV in the left MPFC/dACC and was related to pronounced nodal properties patterns mainly in default mode, sensory, and motor regions; in contrast, PTG was correlated with GMV in the left DLPFC and marginally correlated with a nodal property pattern mainly in emotion regulation-related regions. These findings promote our understanding of the neural substrates of PTSS and PTG, and help to elucidate their relationship. They may also be valuable in suggesting potential brain regions for targeted interventions such as transcranial direct current stimulation (Valero–Cabre et al. 2017; Liu et al. 2022) aimed at decreasing PTSS and increasing PTG in individuals experiencing major trauma events. This is consistent with the purpose of psychoradiology (Lui et al. 2016; Gong 2020; Li et al. 2021).

Acknowledgement

Drs. S. Wang and Q. Gong contributed equally to playing the role of corresponding. We would like to express our deepely thanks to all the participants in this study.

CRediT statement

Huan Lan (Conceptualization, Data curation, Formal analysis, Methodology, Visualization, Writing—original draft), Xueling Suo (Funding acquisition, Methodology, Writing—review & editing), Chao Zuo (Data curation, Investigation), Nanfang Pan (Methodology, Writing—review & editing), Xun Zhang (Methodology, Writing—review & editing), Graham J Kemp (Supervision, Writing—review & editing), Qiyong Gong (Conceptualization, Funding acquisition, Project administration, Resources, Supervision, Writing—review & editing), and Song Wang (Conceptualization, Funding acquisition, Supervision, Writing—review & editing).

Supplementary material

Supplementary material is available at *Cerebral Cortex* online.

Funding

This work was supported by the Key Research and Development Program of Sichuan Province (Grant No. 2023YFS0084), the National Natural Science Foundation of China (Grant Nos. 31800963, 81621003, 81761128023, 81820108018, and 82027808), the National Key R&D Program of China (2022YFC2009900), and the Young Elite Scientists Sponsorship Program by CAST (No. 2022QNRC001).

Conflict of interest statement: None declared.

Data availability

West China Hospital of Sichuan University has an institutional commitment to data-sharing. To get access to the data and comply with the terms of our research ethics committee approval, an application to the corresponding author will be required, specifying the geographical extent of sharing.

References

Akiki TJ, Averill CL, Abdallah CG. A network-based neurobiological model of PTSD: evidence from structural and functional neuroimaging studies. *Curr Psychiatry Rep*. 2017:19(11):81.

Alexandra Kredlow M, Fenster RJ, Laurent ES, Ressler KJ, Phelps EA. Prefrontal cortex, amygdala, and threat processing: implications for PTSD. *Neuropsychopharmacology*. 2022:47(1):247–259.

Ashburner J. A fast diffeomorphic image registration algorithm. *NeuroImage*. 2007:38(1):95–113.

Ashburner J, Friston KJ. Voxel-based morphometry–the methods. *NeuroImage*. 2000:11(6 Pt 1):805–821.

Aupperle RL, Allard CB, Grimes EM, Simmons AN, Flagan T, Behrooznia M, Cissell SH, Twamley EW, Thorp SR, Norman SB, et al. Dorsolateral prefrontal cortex activation during emotional anticipation and neuropsychological performance in posttraumatic stress disorder. *Arch Gen Psychiatry*. 2012:69(4):360–371.

Badre D, Wagner AD. Selection, integration, and conflict monitoring; assessing the nature and generality of prefrontal cognitive control mechanisms. *Neuron*. 2004:41(3):473–487.

Balters S, Li R, Espil FM, Piccirilli A, Liu N, Gundran A, Carrion VG, Weems CF, Cohen JA, Reiss AL. Functional near-infrared spectroscopy brain imaging predicts symptom severity in youth exposed to traumatic stress. *J Psychiatr Res*. 2021:144:494–502.

Bao W, Gao Y, Cao L, Li H, Liu J, Liang K, Hu X, Zhang L, Hu X, Gong Q, et al. Alterations in large-scale functional networks in adult posttraumatic stress disorder: a systematic review and meta-analysis of resting-state functional connectivity studies. *Neurosci Biobehav Rev*. 2021:131:1027–1036.

Boggio PS, Rocha M, Oliveira MO, Fecteau S, Cohen RB, Campanha C, Ferreira-Santos E, Meleiro A, Corchs F, Zaghi S, et al. Noninvasive brain stimulation with high-frequency and low-intensity repetitive transcranial magnetic stimulation treatment for posttraumatic stress disorder. *J Clin Psychiatry*. 2010:71(8):992–999.

Bromis K, Calem M, Reinders A, Williams SCR, Kempton MJ. Meta-analysis of 89 structural MRI studies in posttraumatic stress disorder and comparison with major depressive disorder. *Am J Psychiatry*. 2018:175(10):989–998.

Brooks SK, Webster RK, Smith LE, Woodland L, Wessely S, Greenberg N, Rubin GJ. The psychological impact of quarantine and how to reduce it: rapid review of the evidence. *Lancet*. 2020:395(10227):912–920.

Bullmore E, Sporns O. The economy of brain network organization. *Nat Rev Neurosci*. 2012:13(5):336–349.

Cai M, Ma J, Wang Z, Zhao Y, Zhang Y, Wang H, Xue H, Chen Y, Zhang Y, Wang C, et al. Individual-level brain morphological similarity networks: current methodologies and applications. *CNS Neurosci Ther*. 2023. https://doi.org/10.1111/cns.14384.

Carmassi C, Foghi C, Dell'Oste V, Cordone A, Bertelloni CA, Bui E, Dell'Osso L. PTSD symptoms in healthcare workers facing the three coronavirus outbreaks: what can we expect after the COVID-19 pandemic. *Psychiatry Res*. 2020:292:113312.

Carrion VG, Garrett A, Menon V, Weems CF, Reiss AL. Posttraumatic stress symptoms and brain function during a response-inhibition task: an fMRI study in youth. *Depress Anxiety*. 2008:25(6):514–526.

Carrion VG, Weems CF, Richert K, Hoffman BC, Reiss AL. Decreased prefrontal cortical volume associated with increased bedtime cortisol in traumatized youth. *Biol Psychiatry*. 2010:68(5):491–493.

Cordova MJ, Cunningham LL, Carlson CR, Andrykowski MA. Posttraumatic growth following breast cancer: a controlled comparison study. *Health Psychol*. 2001:20(3):176–185.

Creamer M, Bell R, Failla S. Psychometric properties of the impact of event scale - revised. *Behav Res Ther*. 2003:41(12):1489–1496.

Cui PP, Wang PP, Wang K, Ping Z, Wang P, Chen C. Post-traumatic growth and influencing factors among frontline nurses fighting against COVID-19. *Occup Environ Med*. 2021:78(2):129–135.

Dekel S, Ein-Dor T, Solomon Z. Posttraumatic growth and posttraumatic distress: a longitudinal study. *Psychol Trauma*. 2012:4(1):94–101.

Elzinga BM, Bremner JD. Are the neural substrates of memory the final common pathway in posttraumatic stress disorder (PTSD)? *J Affect Disord*. 2002:70(1):1–17.

Faul F, Erdfelder E, Lang AG, Buchner A. G*Power 3: a flexible statistical power analysis program for the social, behavioral, and biomedical sciences. *Behav Res Methods*. 2007:39(2):175–191.

Foulkes L, Blakemore SJ. Studying individual differences in human adolescent brain development. *Nat Neurosci*. 2018:21(3):315–323.

Fujisawa TX, Jung M, Kojima M, Saito DN, Kosaka H, Tomoda A. Neural basis of psychological growth following adverse experiences: a resting-state functional MRI study. *PLoS One*. 2015:10(8):e0136427.

Garrett AS, Carrion V, Kletter H, Karchemskiy A, Weems CF, Reiss A. Brain activation to facial expressions in youth with PTSD symptoms. *Depress Anxiety*. 2012:29(5):449–459.

Genon S, Eickhoff SB, Kharabian S. Linking interindividual variability in brain structure to behaviour. *Nat Rev Neurosci*. 2022:23(5):307–318.

Gong Q. *Psychoradiology, neuroimaging clinics of North America*. Vol. 30. New York: Elsevier Inc; 2020 pp. 1–123.

Groarke A, Curtis R, Groarke JM, Hogan MJ, Gibbons A, Kerin M. Posttraumatic growth in breast cancer: how and when do distress and stress contribute? *Psychooncology*. 2017:26(7):967–974.

Gross JJ, John OP. Individual differences in two emotion regulation processes: implications for affect, relationships, and well-being. *J Pers Soc Psychol*. 2003:85(2):348–362.

Harnett NG, Finegold KE, Lebois LAM, van Rooij SJH, Ely TD, Murty VP, Jovanovic T, Bruce SE, House SL, Beaudoin FL, et al. Structural covariance of the ventral visual stream predicts posttraumatic intrusion and nightmare symptoms: a multivariate data fusion analysis. *Transl Psychiatry*. 2022:12(1):321.

Herringa RJ, Phillips ML, Fournier JC, Kronhaus DM, Germain A. Childhood and adult trauma both correlate with dorsal anterior cingulate activation to threat in combat veterans. *Psychol Med*. 2013:43(7):1533–1542.

Ho SM, Chan CL, Ho RT. Posttraumatic growth in Chinese cancer survivors. *Psychooncology*. 2004:13(6):377–389.

Jeong H, Lee YJ, Kim N, Jeon S, Jun JY, Yoo SY, Lee SH, Lee J, Kim SJ. Increased medial prefrontal cortical thickness and resilience to traumatic experiences in North Korean refugees. *Sci Rep*. 2021:11(1):14910.

Jessen K, Mandl RCW, Fagerlund B, Bojesen KB, Raghava JM, Obaid HG, Jensen MB, Johansen LB, Nielsen MØ, Pantelis C, et al. Patterns of cortical structures and cognition in antipsychotic-naïve patients with first-episode schizophrenia: a partial least squares correlation analysis. *Biol Psychiatry Cogn Neurosci Neuroimaging*. 2019:4(5):444–453.

Jin Y, Xu J, Liu D. The relationship between post traumatic stress disorder and post traumatic growth: gender differences in PTG and PTSD subgroups. *Soc Psychiatry Psychiatr Epidemiol*. 2014:49(12):1903–1910.

Kaiser RH, Andrews-Hanna JR, Wager TD, Pizzagalli DA. Large-scale network dysfunction in major depressive disorder: a meta-analysis of resting-state functional connectivity. *JAMA Psychiatry*. 2015:72(6):603–611.

Kanai R, Rees G. The structural basis of inter-individual differences in human behaviour and cognition. *Nat Rev Neurosci*. 2011:12(4):231–242.

Ke S, Sun L, Zhou J, Wang Y, Bu T, Chu H, Yang J, Wang W, Wang W, Li J, et al. Factors influencing post-traumatic stress symptoms in Chinese adolescents during the COVID-19 pandemic. *Front Psychiatry*. 2022:13:892014.

Khundrakpam BS, Lewis JD, Reid A, Karama S, Zhao L, Chouinard-Decorte F, Evans AC. Imaging structural covariance in the development of intelligence. *NeuroImage*. 2017:144(Pt A):227–240.

Kong F, Hu S, Xue S, Song Y, Liu J. Extraversion mediates the relationship between structural variations in the dorsolateral prefrontal cortex and social well-being. *NeuroImage*. 2015:105:269–275.

Krawczyk DC. Contributions of the prefrontal cortex to the neural basis of human decision making. *Neurosci Biobehav Rev*. 2002:26(6):631–664.

Krishnan A, Williams LJ, McIntosh AR, Abdi H. Partial Least Squares (PLS) methods for neuroimaging: a tutorial and review. *NeuroImage*. 2011:56(2):455–475.

Lai H, Kong X, Zhao Y, Pan N, Zhang X, He M, Wang S, Gong Q. Patterns of a structural covariance network associated with dispositional optimism during late adolescence. *NeuroImage*. 2022:251:119009.

Lai H, Zhao Y, Li J, Gong Q, Wang S. Neuroanatomical signatures associated with dispositional optimism predict COVID-19-related posttraumatic stress symptoms. *Cereb Cortex*. 2023:33(15):9387–9398.

Li F, Sun H, Biswal BB, Sweeney JA, Gong Q. Artificial intelligence applications in psychoradiology. *Psychoradiology*. 2021:1:94–107.

Li L, Mao M, Wang S, Yin R, Yan H, Jin Y, Cheng Y. Posttraumatic growth in Chinese nurses and general public during the COVID-19 outbreak. *Psychol Health Med*. 2022a:27(2):301–311.

Li L, Zhang Y, Zhao Y, Li Z, Kemp GJ, Wu M, Gong Q. Cortical thickness abnormalities in patients with post-traumatic stress disorder: a vertex-based meta-analysis. *Neurosci Biobehav Rev*. 2022b:134:104519.

Lin J, Li L, Pan N, Liu X, Zhang X, Suo X, Kemp GJ, Wang S, Gong Q. Neural correlates of neuroticism: a coordinate-based meta-analysis of resting-state functional brain imaging studies. *Neurosci Biobehav Rev*. 2023:146:105055.

Liu AN, Wang LL, Li HP, Gong J, Liu XH. Correlation between post-traumatic growth and posttraumatic stress disorder symptoms based on Pearson correlation coefficient: a meta-analysis. *J Nerv Ment Des*. 2017:205(5):380–389.

Liu G, Zeng G, Wang F, Rotshtein P, Peng K, Sui J. Praising others differently: neuroanatomical correlates to individual differences in trait gratitude and elevation. *Soc Cogn Affect Neurosci*. 2018:13(12):1225–1234.

Liu C, Han T, Xu Z, Liu J, Zhang M, Du J, Zhou Q, Duan Y, Li Y, Wang J, et al. Modulating gamma oscillations promotes brain connectivity to improve cognitive impairment. *Cereb Cortex*. 2022:32(12):2644–2656.

Liu X, Zhao Y, Suo X, Zhang X, Pan N, Kemp GJ, Gong Q, Wang S. Psychological resilience mediates the protective role of default-mode network functional connectivity against COVID-19 vicarious traumatization. *Transl Psychiatry*. 2023:13(1):231.

Logue MW, van Rooij SJH, Dennis EL, Davis SL, Hayes JP, Stevens JS, Densmore M, Haswell CC, Ipser J, Koch SBJ, et al. Smaller hippocampal volume in posttraumatic stress disorder: a multisite ENIGMA-PGC study: subcortical volumetry results from posttraumatic stress disorder consortia. *Biol Psychiatry*. 2018:83(3):244–253.

Lu F, Cui Q, Chen Y, He Z, Sheng W, Tang Q, Yang Y, Luo W, Yu Y, Chen J, et al. Insular-associated causal network of structural covariance evaluating progressive gray matter changes in major depressive disorder. *Cereb Cortex*. 2023:33(3):831–843.

Lui S, Zhou XJ, Sweeney JA, Gong Q. Psychoradiology: the frontier of neuroimaging in psychiatry. *Radiology*. 2016:281(2):357–372.

Lyoo IK, Kim JE, Yoon SJ, Hwang J, Bae S, Kim DJ. The neurobiological role of the dorsolateral prefrontal cortex in recovery from trauma. Longitudinal brain imaging study among survivors of the South Korean subway disaster. *Arch Gen Psychiatry*. 2011:68(7):701–713.

MacDonald AW 3rd, Cohen JD, Stenger VA, Carter CS. Dissociating the role of the dorsolateral prefrontal and anterior cingulate cortex in cognitive control. *Science*. 2000:288(5472):1835–1838.

Marek S, Tervo-Clemmens B, Calabro FJ, Montez DF, Kay BP, Hatoum AS, Donohue MR, Foran W, Miller RL, Hendrickson TJ, et al. Reproducible brain-wide association studies require thousands of individuals. *Nature*. 2022:603(7902):654–660.

Marziliano A, Tuman M, Moyer A. The relationship between post-traumatic stress and post-traumatic growth in cancer patients and survivors: a systematic review and meta-analysis. *Psychooncology*. 2020:29(4):604–616.

Mo Y, Tao P, Liu G, Chen L, Li G, Lu S, Zhang G, Liang R, Huang H. Post-traumatic growth of nurses who faced the COVID-19 epidemic and its correlation with professional self-identity and social support. *Front Psychiatry*. 2021:12:562938.

Morawetz C, Riedel MC, Salo T, Berboth S, Eickhoff SB, Laird AR, Kohn N. Multiple large-scale neural networks underlying emotion regulation. *Neurosci Biobehav Rev*. 2020:116:382–395.

Nakagawa S, Sugiura M, Sekiguchi A, Kotozaki Y, Miyauchi CM, Hanawa S, Araki T, Takeuchi H, Sakuma A, Taki Y, et al. Effects of post-traumatic growth on the dorsolateral prefrontal cortex after a disaster. *Sci Rep*. 2016:6:34364.

Nosek BA, Hardwicke TE, Moshontz H, Allard A, Corker KS, Dreber A, Fidler F, Hilgard J, Kline Struhl M, Nuijten MB, et al. Replicability, robustness, and reproducibility in psychological science. *Annu Rev Psychol*. 2022:73:719–748.

Pan N, Wang S, Zhao Y, Lai H, Qin K, Li J, Biswal BB, Sweeney JA, Gong Q. Brain gray matter structures associated with trait impulsivity: a systematic review and voxel-based meta-analysis. *Hum Brain Mapp*. 2021:42(7):2214–2235.

Pan N, Qin K, Yu Y, Long Y, Zhang X, He M, Suo X, Zhang S, Sweeney JA, Wang S, et al. Pre-COVID brain functional connectome features prospectively predict emergence of distress symptoms after onset of the COVID-19 pandemic. *Psychol Med*. 2023:53(11):5155–66.

Pan N, Yang C, Suo X, Shekara A, Hu S, Gong Q, Wang S. Sex differences in the relationship between brain gray matter volume and psychological resilience in late adolescence. *Eur Child Adolesc Psychiatry*. 2023. https://doi.org/10.1007/s00787-023-02231-7.

Patel R, Spreng RN, Shin LM, Girard TA. Neurocircuitry models of posttraumatic stress disorder and beyond: a meta-analysis of functional neuroimaging studies. *Neurosci Biobehav Rev*. 2012:36(9):2130–2142.

Paus T. Mapping brain maturation and cognitive development during adolescence. *Trends Cognit Sci*. 2005:9(2):60–68.

Peng M, Mo B, Liu Y, Xu M, Song X, Liu L, Fang Y, Guo T, Ye J, Yu Z, et al. Prevalence, risk factors and clinical correlates of depression in quarantined population during the COVID-19 outbreak. *J Affect Disord*. 2020:275:119–124.

Pfefferbaum B, North CS. Mental health and the Covid-19 pandemic. *N Engl J Med*. 2020:383(6):510–512.

Pietrzak RH, Tsai J, Southwick SM. Association of symptoms of posttraumatic stress disorder with posttraumatic psychological growth among US veterans during the COVID-19 pandemic. *JAMA Netw Open*. 2021:4(4):e214972.

Pitman RK, Rasmusson AM, Koenen KC, Shin LM, Orr SP, Gilbertson MW, Milad MR, Liberzon I. Biological studies of post-traumatic stress disorder. *Nat Rev Neurosci*. 2012:13(11):769–787.

Podsakoff PM, MacKenzie SB, Lee JY, Podsakoff NP. Common method biases in behavioral research: a critical review of the literature and recommended remedies. *J Appl Psychol*. 2003:88(5):879–903.

Pozzi E, Vijayakumar N, Rakesh D, Whittle S. Neural correlates of emotion regulation in adolescents and emerging adults: a meta-analytic study. *Biol Psychiatry*. 2021:89(2):194–204.

Qiu J, Xia Y, He L, Chen Q, Sang N, Liu W, Li H. Abnormal rsFC and GMV changes in parahippocampal and DLPFC for high Deja vu experienced subjects. *Biol Psychol*. 2018:133:72–78.

Rauch SL, Shin LM, Phelps EA. Neurocircuitry models of post-traumatic stress disorder and extinction: human neuroimaging research–past, present, and future. *Biol Psychiatry*. 2006:60(4):376–382.

Rossi R, Socci V, Talevi D, Mensi S, Niolu C, Pacitti F, Di Marco A, Rossi A, Siracusano A, Di Lorenzo G. COVID-19 pandemic and lockdown measures impact on mental health among the general population in Italy. *Front Psychiatry*. 2020:11:790.

Schou TM, Joca S, Wegener G, Bay-Richter C. Psychiatric and neuropsychiatric sequelae of COVID-19 - a systematic review. *Brain Behav Immun*. 2021:97:328–348.

Shakespeare-Finch J, Lurie-Beck J. A meta-analytic clarification of the relationship between posttraumatic growth and symptoms of posttraumatic distress disorder. *J Anxiety Disord*. 2014:28(2):223–229.

Shanahan L, Steinhoff A, Bechtiger L, Murray AL, Nivette A, Hepp U, Ribeaud D, Eisner M. Emotional distress in young adults during the COVID-19 pandemic: evidence of risk and resilience from a longitudinal cohort study. *Psychol Med*. 2022:52(5):824–833.

Shand LK, Cowlishaw S, Brooker JE, Burney S, Ricciardelli LA. Correlates of post-traumatic stress symptoms and growth in cancer patients: a systematic review and meta-analysis. *Psychooncology*. 2015:24(6):624–634.

Smallwood J, Bernhardt BC, Leech R, Bzdok D, Jefferies E, Margulies DS. The default mode network in cognition: a topographical perspective. *Nat Rev Neurosci*. 2021:22(8):503–513.

Solomon Z, Dekel R. Posttraumatic stress disorder and posttraumatic growth among Israeli ex-POWs. *J Trauma Stress*. 2007:20(3):303–312.

Sowell ER, Thompson PM, Tessner KD, Toga AW. Mapping continued brain growth and gray matter density reduction in dorsal frontal cortex: inverse relationships during postadolescent brain maturation. *J Neurosci*. 2001:21(22):8819–8829.

Suo X, Zuo C, Lan H, Pan N, Zhang X, Kemp GJ, Wang S, Gong Q. COVID-19 vicarious traumatization links functional connectome to general distress. *NeuroImage*. 2022:255:119185.

Tedeschi RG, Calhoun LG. The posttraumatic growth inventory: measuring the positive legacy of trauma. *J Trauma Stress*. 1996:9(3):455–471.

Tedeschi RG, Calhoun LG. Posttraumatic growth: conceptual foundations and empirical evidence. *Psychol Inq*. 2004:15(1):1–18.

Tsai J, El-Gabalawy R, Sledge WH, Southwick SM, Pietrzak RH. Post-traumatic growth among veterans in the USA: results from the National Health and Resilience in Veterans Study. *Psychol Med*. 2015:45(1):165–179.

Tu Y, Zhang Y, Li Y, Zhao Q, Bi Y, Lu X, Kong Y, Wang L, Lu Z, Hu L. Post-traumatic stress symptoms in COVID-19 survivors: a self-report and brain imaging follow-up study. *Mol Psychiatry*. 2021:26(12):7475–7480.

Tzourio-Mazoyer N, Landeau B, Papathanassiou D, Crivello F, Etard O, Delcroix N, Mazoyer B, Joliot M. Automated anatomical labeling of activations in SPM using a macroscopic anatomical parcellation of the MNI MRI single-subject brain. *NeuroImage*. 2002:15(1):273–289.

Valero-Cabre A, Amengual JL, Stengel C, Pascual-Leone A, Coubard OA. Transcranial magnetic stimulation in basic and clinical neuroscience: a comprehensive review of fundamental principles and novel insights. *Neurosci Biobehav Rev*. 2017:83:381–404.

Vindegaard N, Benros ME. COVID-19 pandemic and mental health consequences: systematic review of the current evidence. *Brain Behav Immun*. 2020:89:531–542.

Wang J, Wang X, Xia M, Liao X, Evans A, He Y. GRETNA: a graph theoretical network analysis toolbox for imaging connectomics. *Front Hum Neurosci*. 2015:9:386.

Wang H, Jin X, Zhang Y, Wang J. Single-subject morphological brain networks: connectivity mapping, topological characterization and test-retest reliability. *Brain Behav*. 2016:6(4):e00448.

Wang S, Dai J, Li J, Wang X, Chen T, Yang X, He M, Gong Q. Neuroanatomical correlates of grit: growth mindset mediates the association between gray matter structure and trait grit in late adolescence. *Hum Brain Mapp*. 2018:39(4):1688–1699.

Wang C, Pan R, Wan X, Tan Y, Xu L, McIntyre RS, Choo FN, Tran B, Ho R, Sharma VK, et al. A longitudinal study on the mental health of general population during the COVID-19 epidemic in China. *Brain Behav Immun*. 2020a:87:40–48.

Wang S, Zhao Y, Li J, Lai H, Qiu C, Pan N, Gong Q. Neurostructural correlates of hope: dispositional hope mediates the impact of the SMA gray matter volume on subjective well-being in late adolescence. *Soc Cogn Affect Neurosci*. 2020b:15(4):395–404.

Wang S, Zhao Y, Li J. True grit and brain: trait grit mediates the connection of DLPFC functional connectivity density to post-traumatic growth following COVID-19. *J Affect Disord*. 2023:325:313–320.

Wei C, Han J, Zhang Y, Hannak W, Dai Y, Liu Z. Affective emotion increases heart rate variability and activates left dorsolateral prefrontal cortex in post-traumatic growth. *Sci Rep*. 2017a:7(1):16667.

Wei C, Han J, Zhang Y, Hannak W, Liu Z. The characteristics of emotional response of post-traumatic stress disorder and post-traumatic growth among Chinese adults exposed to an explosion incident. *Front Public Health*. 2017b:5:3.

Worsley KJ, Evans AC, Marrett S, Neelin P. A three-dimensional statistical analysis for CBF activation studies in human brain. *J Cereb Blood Flow Metab*. 1992:12(6):900–918.

Wu Z, Xu J, Sui Y. Posttraumatic stress disorder and posttraumatic growth coexistence and the risk factors in Wenchuan earthquake survivors. *Psychiatry Res*. 2016:237:49–54.

Xu T, Chen F, Zhang L, Dai Y, Ke J, Qi R, Lu G, Zhong Y. Study on the changes of structural covariance network in post-traumatic stress disorder. *Brain Imaging Behav*. 2022:16(5):1992–2000.

Yamasue H, Abe O, Suga M, Yamada H, Rogers MA, Aoki S, Kato N, Kasai K. Sex-linked neuroanatomical basis of human altruistic cooperativeness. *Cereb Cortex*. 2008:18(10):2331–2340.

Yan S, Yang J, Ye M, Chen S, Xie C, Huang J, Liu H. Post-traumatic growth and related influencing factors in discharged COVID-19 patients: a cross-sectional study. *Front Psychol*. 2021:12:658307.

Zhang J, Wang J, Wu Q, Kuang W, Huang X, He Y, Gong Q. Disrupted brain connectivity networks in drug-naive, first-episode major depressive disorder. *Biol Psychiatry*. 2011:70(4):334–342.

Zhang X, Zhang J, Wang L, Zhang W. Altered gray matter volume and its correlation with PTSD severity in Chinese earthquake survivors. *Front Psychiatry*. 2018:9:629.